Journal of Applied Mechanics and Technical Physics, Vol. 39, No. 3, 1998

GRAVITY-FLOW STRUCTURE IN A MISCIBLE FLUID

V. Yu. Liapidevskii

UDC 532.526

Steady-state density flows in a horizontal channel are studied based on a two-layer shallow water model, developed by the author, with allowance for the mixing between the layers. The structure of a gravity flow and the intensity of mixing in the flow head are shown to depend significantly on the channel depth. Conditions behind the flow front, which determine the basic characteristics of a gravity flow, are found.

The gravity or "density" flow is a flow of one fluid inside another under the action of gravity forces. Usually, this flow occurs along the upper or lower boundary, but it can also occur as intrusions along the interface of liquids of different density. An important aspect of a gravity flow that determines its structure is the intense mixing immediately behind the front.

In a long-wave approximation, the three-layer flow pattern which includes not only homogeneous layers of different density but also a region occupied by a mixed fluid is the most appropriate model for the class of flows considered. Three-layer flow equations which describe the mixing and generation of short waves at the internal boundaries of the layers were derived and analyzed in [1, 2]. Introduction of an interlayer between homogeneous layers into a mathematical model as a domain with a particular set of averaged quantities which characterize this domain (density, thickness, velocity, etc.) is based on the use of the total laws of conservation of mass, momentum, and energy, and this allows one to take account of the effect of the second mode (interlayer waves) on the structure of a gravity flow. This effect has been studied poorly, and it should be taken into account in the interpretation of laboratory and field observations.

Another distinctive feature of a gravity flow — the formation of a special "nose" at the leading front — is associated with the effect of the boundary layer [3], and we omit it in the present paper. In comparing the results obtained with experimental data, attention was mainly given to flow patterns with a "moving" bottom. This pattern was implemented by Simpson and Britter [4] and Garcia and Parsons [5]. In these studies, the "slip" conditions were effectively simulated, and the stationary front of a gravity flow interacted with a homogeneous upstream flow.

In the present paper, a regime of maximum entrainment is shown to occur downstream the gravity-flow front in the absence of additional control. In addition, it is shown that the basic flow characteristics, including the internal Richardson number in the mixing region, the amount of a mixed liquid, etc., can be found as functions of only two dimensionless parameters, namely, the Froude number of an incoming flow and the difference between the heads in counterflows.

1. Let a channel with a horizontal bottom be filled with a two-layer liquid of depth H, the upper homogeneous layer of thickness h^+ and density ρ^+ being separated from the lower homogeneous layer of depth h and density ρ^- ($\rho^+ < \rho^-$) by an interlayer of thickness η ($h + \eta + h^+ = H$). An intense small-scale motion with root-mean-square velocity q develops in the layers owing to the velocity shear and, as a result of this motion, the mean density $\bar{\rho}$ in the interlayer differs from the density of the homogeneous layers. With

Lavrent'ev Institute of Hydrodynamics, Siberian Division, Russian Academy of Sciences, Novosibirsk 630090. Translated from Prikladnaya Mekhanika i Tekhnicheskaya Fizika, Vol. 39, No. 3, pp. 79–85, May–June, 1998. Original article submitted September 23, 1996; revision submitted January 30, 1997.

0021-8944/98/3903-0393 $20.00

allowance for mixing, in the Boussinesq approximation $[(\rho^- - \rho^+)/\rho^+ \ll 1]$ the equations of a plane-parallel flow are of the form

$$
\begin{gathered}
h_t + (hu)_x = -\sigma q, \quad h_t^+ + (h^+ w)_x = -\sigma q, \quad \eta_t + (\eta v)_x = 2\sigma q, \\
w_t + (w^2/2 + p)_x = 0, \quad u_t + (u^2/2 + bh + \bar{b}\eta + p)_x = 0, \\
(hu + \eta v + h^+ w)_t + (hu^2 + \eta v^2 + h^+ w^2 + Hp + \bar{b}\eta^2/2 + \bar{b}\eta h + bh^2/2)_x = 0, \\
(bh + \bar{b}\eta)_t + (bhu + \bar{b}\eta v)_x = 0, \\
(hu^2 + \eta(v^2 + q^2) + h^+ w^2 + \bar{b}\eta^2 + 2\bar{b}\eta h + bh^2)_t \\
+ (hu^3 + \eta v(v^2 + q^2) + h^+ w^3 + 2p\bar{Q} + 2\bar{b}\eta hu + 2\bar{b}(h + \eta)\eta v + 2bh^2 u)_x = 0.
\end{gathered}
\tag{1.1}
$$

Here $\bar{b} = (\bar{\rho} - \rho^+)g/\rho^+$, $b = (\rho^- - \rho^+)g/\rho^+$ is the buoyancy in the interlayer and the lower layer, g is the acceleration of gravity, u, w, and v are the mean horizontal velocities in the upper and lower layers and the interlayer, respectively, and $\rho^+ p$ is the pressure at the upper flow boundary ($H \equiv$ const in the Boussinesq approximation). By virtue of Eqs. (1.1), the total flow rate $\bar{Q} = hu + \eta v + h^+ w$ is only a function of time, and it is considered to be prescribed from the boundary conditions.

System (1.1) is derived by the addition of the total laws of conservation of mass, momentum, and energy, which are necessary to find the quantities v, $\bar{b}$, and q in the layer [2], to the well-known "shallow water" equations for the upper and lower homogeneous layers.

The law of energy conservation is used to determine the rate of entrainment of a liquid from homogeneous layers into the interlayer. The entrainment rate is assumed here to be proportional to the velocity q of small-scale motion in the interlayer [6].

The numerical value of the coefficient $\sigma = 0.15$ determines the relationship between the vertical and horizontal scales of flow, and it is not important for the model because the parameter σ can be excluded from Eqs. (1.1) by replacing the variables.

Equations (1.1) are most suitable for describing entrainment processes into the interlayer that are due to the development of the Kelvin–Helmholtz instability at the interface of homogeneous layers in flows with velocity shear. This model and its modifications were used in the problems of the evolution of a mixing layer [1, 2], its transition to a submerged jet, and also in the problem of flow blocking in a supercritical flow of a two-layer miscible liquid over an obstacle.

System (1.1) is written in the form of conservation laws, because the three-layer flow pattern solves the well-known problem of the choice of relations on inner hydraulic jumps. As was shown in [1, 2], the structure of the equations is such that, for a mixing layer and a submerged jet, the regime of maximum entrainment [7] is realized by virtue of the equations without additional assumptions on the internal flow stability.

In (1.1), the desired functions are h, η, u, v, w, $\bar{b}$, q, and p. The characteristics of the system consists of the characteristics of the well-known system of three-layer shallow-water equations and the multiple contact characteristic $dx/dt = v$. Therefore, system (1.1) is hyperbolic for an insignificant velocity shear in the layers. The model considered also incorporates the mechanism of entrainment of a fluid from homogeneous layers into an interlayer owing to the conversion of the kinetic energy of the flow to the energy of vortex motion. Therefore, with increase in the velocity shear in the layers, the interlayer thickness also increases, which does not allow the solution of system (1.1) to go beyond the hyperbolicity domain. Flow deformation in the inner hydraulic jumps occurs so rapidly that one can ignore the entrainment caused by the instability of the front. In view of this, the hyperbolicity of the system of equations immediately behind the front is an additional condition for jump stability.

For the gravitational flows considered below, an analysis of relations on the jumps is complicated by the fact that, in a stationary flow, the particles from the homogeneous layers arrive at the mixing region from different sides. This means that in the gravity-flow front, the discontinuities that correspond to the first and second modes merge. The problem of stability of such formations has not yet been analyzed adequately. Nevertheless, many characteristic properties of gravity flow can be obtained from the subsequent analysis of stationary solutions of system (1.1).

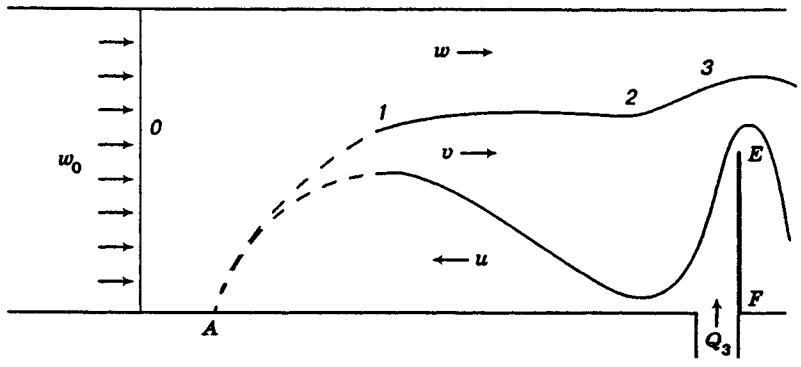

Fig. 1

2. We shall consider the gravity-flow pattern realized in [4, 5] (Fig. 1). A homogeneous flow of a liquid of density ρ^+ moving in a positive direction with horizontal velocity $w_0 > 0$ was created in a horizontal channel. After that, a liquid with density ρ^- ($\rho^+ < \rho^-$) was fed into the channel. Propagating upstream of a homogeneous flow, this liquid formed a steady-state front of the gravity flow. To eliminate the effect of friction and to create a uniformly incoming flow on the left of the front (point A), use was made of a "bottom" moving with velocity w_0 in the experiments of [4, 5].

Figure 1 shows the structure of the leading section of a gravity flow. One can distinguish in it a frontal part (the dashed curve) with a distinct smooth interface between the liquids of different density. In practice, no mixing occurs in this section and, owing to large vertical gradients, the hypothesis of a hydrostatic pressure distribution in the vicinity of the interface is not fulfilled. Therefore, the frontal part of the gravity flow in the shallow-water approximation is modeled by an internal hydraulic jump transforming state 0 into equilibrium state 1 behind the flow front. An intense development of the shear instability is observed in the 1–2 section, and this leads to the formation of vortices and the entrainment of the liquid from the homogeneous layers into the interlayer. The flow rate Q_3 in the lower layer, which is necessary for sustaining a steady-state flow, is determined precisely in this section.

The inner hydraulic jump (the 2–3 transition), which corresponds to the second mode, is not distinct in the experiments. Its occurrence is primarily connected with additional conditions of flow control at the channel exit, in particular, with the height of the barrier EF, which limits the outflow from the lower layer downstream. As a subsequent analysis of steady-state solutions of system (1.1) shows, the jump can be absent altogether. In this case, the regime of maximal entrainment at which the change in the conditions at the exit has no effect on the flow structure is realized.

To determine the basic flow parameters in the 0–3 section, we use steady-state solutions of system (1.1). The homogeneous conservation laws yield the following integrals:

$$\begin{gathered} hu + \eta v/2 = 0, \quad h^+ w + \eta v/2 = H w_0, \quad b h u + \bar{b}\eta v = 0, \\ w^2/2 + p = w_0^2/2 + p_0 = J^+, u^2/2 + bh + \bar{b}\eta + p = J^-, \\ hu^2 + \eta v^2 + h^+ w^2 + \bar{b}\eta^2/2 + \bar{b}h\eta + bh^2/2 + pH = H w_0^2 + p_0 H, \\ hu^3 + \eta v(v^2 + q^2) + h^+ w^3 + 2pH w_0 + 2\bar{b}\eta h u + 2\bar{b}(h + \eta)\eta v + 2bh^2 u = H w_0^3 + 2p_0 H w_0. \end{gathered} \tag{2.1}$$

Relations (2.1) hold both in the domain of continuous variation of the flow parameters in the 1–2 section and on the inner hydraulic jumps (the 0–1 and 2–3 transitions). The Froude number of an incoming flow $\mathrm{Fr} = w_0/\sqrt{bH}$ and the total head difference $\Delta J = (J^- - J^+)/(bH)$ are assumed to be the basic dimensionless parameters. In system (2.1), the desired quantities are h, η, u, v, w, q^2, $p - p_0$, and $\bar{b}$, i.e., solutions (2.1) form a one-parameter family. On the inner hydraulic jumps, entrainment can be ignored, which produces additional relations $\eta_1 v_1 = 0$ and $\eta_2 v_2 = \eta_3 v_3$. One can choose the flow rate in the lower layer $Q = -hu = \eta v/2$ as an independent parameter which characterizes the state of the flow in the 1–2 section. By virtue of (2.1),

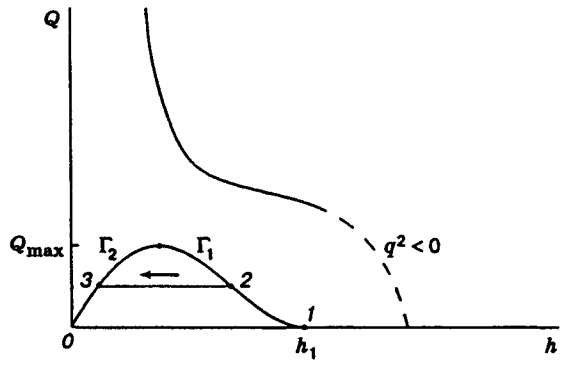

Fig. 2

$(b-2\bar{b})Q=0$, and, therefore, for $Q>0$ we have $\bar{b}=b/2$.

For Froude numbers from the interval $0<\mathrm{Fr}<0.5$ and sufficiently small positive values of the parameter ΔJ, the dependence $h=h(Q)$ is depicted in Fig. 2.[1] The dashed curve shows a physically inadmissible branch of solution (2.1) with $q^2<0$. For $Q<Q_{\max}$, there are two branches Γ_1 and Γ_2, which merge for $Q=Q_{\max}$. The solution is transformed by a hydraulic jump from state 0 to state 1 for $Q_1=0$ and $h_1>0$, i.e., $u_1=v_1=0$ and $\eta_1>0$. The part of the curve Γ_1 between points 1 and 2 corresponds to the possible states in the 1–2 section of the flow (Fig. 1), where the quantity Q monotonically increases due to entrainment. The thickness of the lower layer h decreases, and the total thickness of the homogeneous and mixed layers $h+\eta$ remains almost constant, which was noted in the experiments described in [4, 5]. Next, the transition (shown by the arrow) from state 2 to state 3 on the curve Γ_2 is possible by means of a hydraulic jump for $Q_3=Q_2$. This transition is the internal hydraulic jump of the second mode, because system (1.1) is hyperbolic in state 3, i.e., there are four different roots of the characteristic polynomial, two of them being positive and the other two being negative.

The velocity of propagation of the characteristics λ_i $(i=1,2,3,4)$ is determined by the roots of the characteristic polynomials $\Delta(\lambda)$ on solution (1.1), where

$$\Delta(\lambda)=\left(\frac{(u-\lambda)^2}{bh}+\frac{(v-\lambda)^2}{b\eta}-\frac{1}{2}\right)\left(\frac{(w-\lambda)^2}{bh^+}+\frac{(v-\lambda)^2}{b\eta}-\frac{1}{2}\right)-\frac{(v-\lambda)^4}{b^2\eta^2}.$$

We have $\Delta(0)<0$ in the curve Γ_1 and $\Delta(0)>0$ in the curve Γ_2; note that $\lambda_1<\lambda_2<0<\lambda_3<\lambda_4$. Therefore, $\Delta(0)=0$ for $Q=Q_{\max}$, i.e., the critical flow that corresponds to a regime of maximal entrainment occurs. This regime is realized when the 2–3 transition, which is due to additional control at the channel exit, in particular, the effect of the additional barrier EF, is absent.

Precisely the critical regime of maximum entrainment is reached in the experiments described in [4], because the authors noted the nondependence of the flow structure on the boundary conditions. In this case, the flow rate Q_3 in the lower layer coincides with $Q_{\max}$, and it can be determined for known values of Fr and ΔJ.

Similarly to [8], the theoretical analysis of the gravity-flow structure performed in [4] was based on the use of the total laws of conservation of mass and momentum and also the Bernoulli integral in the upper layer for direct determination of the 0–3 transition. The presence of the mixing layer is taken into account by the experimentally found "universal" velocity profile in state 3. The Froude number Fr and the dimensionless flow rate $q=bQ_3/w_0^3$ were chosen as governing parameters.

The quantity q is as a matter of fact the functional of a steady-state flow, and it is impossible to specify it *a priori*. Therefore, the hypothesis of the internal constant Richardson number Ri_L in the interlayer between

[1] Points in Fig. 2 correspond to the flow states in the channel indicated in Fig. 1.

TABLE 1

Fr	ΔJ	q	Ri_L	h_1/H	$(h_1+\eta_1)/H$	h_2/H	$(h_2+\eta_2)/H$	$u_2/\sqrt{bH}$	$v_2/\sqrt{bH}$
0.35	0.05	0.2	0.61	0.1	0.52	0.055	0.52	−0.16	0.039
	0.03	0.09	0.7	0.058	0.51	0.033	0.51	−0.12	0.017
0.40	0.03	0.21	0.48	0.15	0.46	0.074	0.46	−0.18	0.072
	0.02	0.16	0.5	0.12	0.45	0.061	0.48	−0.17	0.054
	0.01	0.12	0.53	0.094	0.45	0.049	0.44	−0.15	0.038
	0	0.078	0.57	0.068	0.44	0.037	0.44	−0.13	0.025
0.45	0.03	0.41	0.3	0.3	0.47	0.16	0.49	−0.24	0.23
	0.02	0.3	0.33	0.25	0.48	0.12	0.44	−0.22	0.17
	0.01	0.23	0.36	0.21	0.43	0.1	0.41	−0.2	0.13
	0	0.17	0.38	0.17	0.41	0.081	0.39	−0.19	0.1
0.48	0.005	0.35	0.27	0.31	0.44	0.17	0.46	−0.23	0.26
	0	0.28	0.28	0.28	0.43	0.14	0.43	−0.22	0.26

homogeneous layers, which is based on experimental observations, was also used as the closure relation:

$$\mathrm{Ri}_L = \frac{b\eta_3}{(w_3 - u_3)^2} = 0.35 \pm 0.1.$$

For specified Fr and Ri_L numbers, the basic flow parameters behind the gravity-flow front, including q, can be uniquely defined.

It is noteworthy that the model considered in [4] is in fact the model of a two-layer flow with allowance for the real velocity profile in the lower layer. Therefore, the effect of the second mode on the flow structure cannot be included into it, although this effect can turn out to be very significant. The appearance of the second-mode hydraulic jump (the 2–3 transition in Figs. 1 and 2) causes a decrease in the flow rate q behind the wave front and an abrupt decrease in the thickness h of the lower layer. A similar mechanism of the action of the downstream conditions on the formation of a mixing layer was studied experimentally and theoretically in [9] and also in [10] with the use of the three-layer flow model (1.1).

Unfortunately, the quantity ΔJ was not measured in [4, 5], but one can make an indirect comparison with experimental data by choosing the quantity ΔJ for a given Fr value such that the dimensionless flow rate of the liquid q in the lower layer is close to experimental data and then by comparing the calculated and observed flow parameters. This is possible only under the assumption that a regime of maximal entrainment is realized, i.e., $Q_3 = Q_{\max}$ (see Fig. 2).

Table 1 shows the basic dimensionless parameters of the gravity flow immediately behind the front (the quantities with subscript 1) and after the reduction of the entrainment process (the quantities with the subscript 2; states 2 and 3 coincide) for various values of the Froude number. The quantities Fr and ΔJ are given, whereas the remaining quantities are calculated using relations (2.1).

It is seen from Table 1 that within the range of experimentally observed values $q = 0.1$–0.3, the Richardson number in the interlayer Ri_L changes relatively little in the neighborhood of $\mathrm{Ri}_L = 0.35$, even for wider limits compared with those postulated in [4]. The range of Froude numbers $0.35 < \mathrm{Fr} < 0.5$ corresponds to the experiments of [4, 5]. For $\mathrm{Fr} > 0.5$ and positive values of ΔJ, the solutions of Eqs. (2.1) with the above indicated properties do not exist. It is noteworthy that the case where $\mathrm{Fr} = 0.5$ and $\Delta J = 0$ is unique, because, for these values of the parameters, the 0–1 transition is described by Benjamin's solution ($\eta_1 = 0$ and $h_1 = 0.5H$) [8], which is the solution of system (2.1) as well.

The solutions of system (2.1) are compared with the experimental data of [5, Table 1a] in Table 2. The quantities q_{exp} and h_{exp} are the experimentally measured values of the flow rate q and the depth of the lower layer h_3. Since the quantity ΔJ was not determined in the experiments of [5], its value was chosen such that

TABLE 2

Experiment number [5]	Fr	q_{exp}	q	ΔJ	h_{exp}/H	h_3/H
1	0.421	0.313	0.315	0.036	0.1	0.11
2	0.358	0.215	0.218	0.048	0.092	0.06
3	0.358	0.165	0.168	0.04	0.077	0.051
4	0.425	0.233	0.23	0.022	0.089	0.088
5	0.368	0.108	0.112	0.025	0.051	0.041
6	0.327	0.132	0.134	0.049	0.053	0.036
7	0.388	0.169	0.165	0.026	0.07	0.057
8	0.448	0.258	0.252	0.015	0.096	0.1

the q and q_{exp} were close for the given Fr number. Here the h_3 values calculated from (2.1) are comparable with those of h_{exp}. The last two columns show that these values are in satisfactory agreement.

Concluding Remarks. (1) The hypothesis of the absence of mixing on the inner hydraulic jumps (the 0–1 and 2–3 transitions) simplifies the model described in this paper. The Kelvin–Helmholtz instability at the interface of liquids of different density begins to develop in the head of the gravity flow before the hydrostatic equilibrium in the flow is reached. However, the inclusion of the effects of nonhydrostatics into the mathematical model gives rise to its pronounced decrease.

(2) In considering unsteady-state flows, for example, in the lock-exchange problem, the influence of the second mode on the gravity-flow structure is manifested only in the case where the velocity of interlayer waves exceeds the velocity of the flow head. Otherwise a regime of maximal entrainment is realized behind the front in which the velocity of interlayer waves coincides with the velocity of the head of a gravity flow.

This work was supported by the Russian Foundation or Fundamental Research (Grant No. 96-01-01641).

REFERENCES

1. V. Yu. Liapidevskii, "Blocking effects in a two-layer flow of an immiscible fluid over an obstacle," *Prikl. Mat. Mekh.*, **58**, No. 4, 108–112 (1994).
2. V. Yu. Liapidevskii, "Model of two-layer shallow water with an irregular interface," in: *Laboratory Modeling of Dynamic Processes in the Ocean* [in Russian], Inst. of Thermal Phys., Sib. Div., Russian Acad. of Sci., Novosibirsk (1991), pp. 87–97.
3. J. E. Simpson and R. E. Britter, "The dynamics of the head of a gravity current advancing over a horizontal surface," *J. Fluid Mech.*, **94**, 477–495 (1979).
4. J. E. Simpson and R. E. Britter, "Experiments on the dynamics of a gravity current head," *J. Fluid Mech.*, **88**, 223–240 (1978).
5. M. H. Garcia and J. D. Parsons, "Mixing at the front of a gravity current," *Proc. 4th Int. Symp. on Stratified Flows* (Grenoble, June 29–July 2, 1994), Vol. 3 (1994).
6. L. V. Ovsyannikov, N. I. Makarenko, V. I. Nalimov, et al., *Nonlinear Problems in the Theory of Surface and Internal Waves* [in Russian], Nauka, Novosibirsk (1985).
7. V. H. Chu and R. E. Baddour, "Turbulent gravity-stratified shear flows," *J. Fluid Mech.*, **138**, 353–378 (1984).
8. T. B. Benjamin, "Gravity currents and related phenomena," *J. Fluid Mech.*, **31**, 209–248 (1968).
9. D. L. Wilkinson and J. R. Wood, "A rapidly varied flow phenomenon in a two-layer flow," *J. Fluid Mech.*, **47**, 241–256 (1971).
10. V. Yu. Liapidevskii, "Mixing and blocking effects in two-layer flow over an obstacle," in: *Proc. 4th Int. Symp. on Stratified Flows* (Grenoble, June 29–July 2, 1994), Vol. 4 (1994).